Published in final edited form as:
Biomaterials. 2011 January ; 32(3): 890–898. doi:10.1016/j.biomaterials.2010.09.053.

Delivery of Rosiglitazone from an Injectable Triple Interpenetrating Network Hydrogel Composed of Naturally Derived Materials

Hanwei Zhang[1], **Aisha Qadeer**[1], **Dennis Mynarcik**[2], and **Weiliam Chen**[1,*]

[1]Division of Wound Healing and Regenerative Medicine, Department of Surgery, New York University School of Medicine, New York, NY10016

[2]Department of Medicine, State University of New York – Stony Brook, Health Science Center, Stony Brook, NY 11794-8154

Abstract

An *in situ* gelable and biodegradable triple-interpenetrating network (3XN) hydrogel, completely devoid of potentially cytotoxic extraneous small molecule crosslinkers, is formulated from partially oxidized dextran (Odex), teleostean and *N*-carboxyethyl chitosan (CEC). Both the rheological profile and mechanical strength of the 3XN hydrogel approximate the combined characteristics of the three individual hydrogels composed of the binary partial formulations (i.e., Odex/CEC, Odex/teleostean, and CEC/teleostean). The 3XN hydrogel is considerably more resistant to fibroblast-mediated degradation compare to each partial formulation in cell culture models; this is attributable to the interpenetrating triple network structure. The presence of teleostean in the 3XN hydrogel imparts cell affinity, constituting an environment amenable to fibroblast growth. *in vivo* subdermal injection into mouse model shows that the 3XN hydrogel does not induce extensive inflammatory response nor is there any evidence of tissue necrosis, further confirming the non-cytotoxicity of the hydrogel and its degradation byproducts. Importantly, the capability of the 3XN hydrogel to serve as a sustained drug delivery vehicle is confirmed using rosiglitazone as a model drug. The presence of rosiglitazone profoundly changes the cell/tissue interactions with the subdermally injected 3XN hydrogel. Rosiglitazone suppresses both the inflammatory response and tissue repair in a dose-dependent manner and considerably moderated the hydrogel degradation.

Keywords

Chitosan; Dextran; Teleostean; Rosiglitazone; Hydrogel; Triple Interpenetrating Network; in situ Gelable

1. Introduction

Numerous studies on adapting hydrogels as biomaterials have been recently reported, in particular, as tissue engineering scaffolds [1–3] and drug delivery systems [4–6]. Hydrogels

*Corresponding Author: Weiliam Chen Division of Wound Healing and Regenerative Medicine NBV-15N1, Department of Surgery New York University School of Medicine New York, NY10016 Tel: 212-263-3002 Fax: 212-263-8216 weiliam.chen@nyumc.org.

could be formulated from both natural [7–10] and synthetic polymers/monomers [11–13]. Comparing with synthetic or semi-synthetic polymers, natural polymers, especially those that are designated by the FDA as *GRAS* (Generally Regarded as Safe), have lower cytotoxicity concerns and thus regulatory hurdles [9,10,14,15]. However, natural polymers generally have considerably weaker mechanical strength and considerably less resistant to degradation; hydrogels formulated from natural materials typically assume these properties, rendering them less appealing for certain biomedical applications. Developing natural material derived *in situ* gelable hydrogels with high mechanical strength and resistant to biodegradation, while avoiding using potentially cytotoxic modifiers, remains a challenge [16–18].

Interpenetrating double networks (DN) is a strategy to enhance the overall mechanical strengths of hydrogels formulated from synthetic or semi-synthetic polymers [19–21]. We have recently reported a hybrid DN photocrosslinked hydrogels composed of *N*, *N*-dimethylacrylamide and modified hyaluronan, which possesses greatly enhanced mechanical properties as compared to the single network hydrogels produced from the individual components [17]. To our knowledge, the current multiple network hydrogels are consisted largely of synthetic polymers or a highly modified natural polymer (i.e., glycidyl methacrylated hyaluronan in our previous study [17]); it has not hitherto been reports describing interpenetrating multiple network hydrogels derived wholly from natural materials.

In this article, we report a class of interpenetrating multiple-networks hydrogels, comprised of minimally modified natural *GRAS* materials, devoid of small molecule crosslinkers. It furthers our previous investigations on various *in situ* gelable single network hydrogels formulated from natural materials including independently, teleostean, oxidized dextran (Odex) and *N*-carboxyethyl chitosan (CEC) [10,22]. By taking advantage of the large disparities of the reaction times between Odex/CEC, CEC/teleostean and Odex/teleostean, a triple interpenetrating network (3XN) Odex/Teleostean/CEC hydrogels is formulated. The rheological behavior of the 3XN hydrogel is an amalgamation of the individual single network hydrogels; it is mechanically strong and more resistant to biodegradation. The non-cytotoxicity of the 3XN hydrogel is also validated in both *in vitro* and *in vivo* models.

The capability of the 3XN hydrogel to serve as an injectable and *in situ* gelable drug delivery vehicle via *ad hoc* blending is demonstrated using rosiglitazone (a thiazolidinedione) as a model drug. Rosiglitazone is a potent high-affinity ligand for the PPAR-γ receptor with efficacies for various conditions including inflammatory processes and tissue repair [23–25], however, systemic administration of rosiglitazone could lead to disconcerting side effects [26]. Skin is one of the most poorly perfused tissues, thus agents systemically administered will likely achieve sub-optimal local concentrations. It was previously shown that thiazolidinedione applied topically was able to inhibit cutaneous inflammation [27]. Mouse subcutaneous model is chosen to investigate the effect of localized delivery of rosiglitazone on inflammatory response and tissue repair; both processes are suppressed by rosiglitazone in a dose-dependent manner.

2. Experiments

2.1. Materials

Dextran (from *Leuconostoc mesenteroides*, M_w=76,000), teleostean, chitosan (deacetylation degree 85%, M_w 750,000), sodium periodate, sodium hydroxide, and acrylic acid were purchased from Sigma-Aldrich (St. Louis, MO). Dialysis tubings (MWCO 3,500 and 6,000) were from Thermo-Fisher (Hampton, NH). Cell culture inserts (polycarbonate, 6.5 mm diameter, 0.2 μm pore size) were purchased from NUNC (Rochester, NY). M. DUNNI

(clone III8C) murine dermal fibroblast CRL-2017 and McCoy's 5A medium were from ATCC (Manassas, VA). Fetal bovine serum (FBS) was acquired from Hyclone (Logan, UT) and Penicillin-Streptomycin (Pen-Strep) solution was from Gibco (Grand Island, NY). MTS assay kits (CellTiter 96s) were from Promega (Madison, WI).

2.2.1 Synthesis of CEC and oxidized dextran (Odex)—CEC was synthesized according to the method we described previously [28]. Briefly, in 50 ml of water containing 1.88 ml of acrylic acid, 1 g of chitosan was dissolved and the mixture was stirred constantly for 3 days while maintained at 50 °C. Thereafter, 10 N aqueous NaOH was added to the reaction mixture to adjust the pH to 10–12. The mixture was dialyzed (MWCO 6,000) extensively against water for 3 days, filtered and then lyophilized to obtain pure CEC. The substitution degree of chitosan undergoing Michael addition reaction was determined as ~45% by ^{1}H NMR. Odex was also prepared by the method we described previously [22]. Briefly, a total of 3.28 g of $NaIO_4$ (dissolved in 100 ml of water) was added to 400 ml of dextran solution (1.25% w/v), after stirred at ambient temperature for 24 h, an equimolar amount of diethylene glycol was added to quench the unreacted $NaIO_4$. The Odex solution was dialyzed exhaustively (MWCO 3,500) for 3 days against water, filtered and pure Odex was obtained by lyophilization. The oxidation degree of dextran was determined by quantifying aldehyde groups formed with tert-butyl carbazate via carbazone formation [22]. The actual oxidation degree of dextran was determined as 20.0%.

2.2.2 Preparation of solutions and formulation of hydrogels—Desired amounts of precursors (Odex, teleostean and CEC) were pre-dissolved in PBS (0.01M, pH=7.4) to form 15, 40 and 5% (w/v) solutions, respectively. The solutions were stored at 5 °C before testing. It should be noted that the teleostean solution remained a flowable liquid at temperatures above 8 °C. Odex/teleostean/CEC hydrogels were prepared by first thoroughly mixing Odex solutions with teleostean solutions, CEC solution was subsequently blended with the Odex/teleostean mixture (the volume ratio of Odex/teleostean /CEC was 2:1:1) by gentle stirring for 10s, the Odex/teleostean/CEC mixture was maintained at 37 °C for rheological characterization.

2.2.3 Rheological measurements—Rheological characterization of hydrogels was performed on a rheometer (HAAKE RS600, Thermo-Fisher, Hampton). All measurements started at t = 60–90 s. For time sweeping tests, the storage moduli G′ and loss moduli G″ of the mixed systems were monitored as functions of time at a frequency of 1 rad/s and a stress strain of 2% under a constant temperature of 37 °C.

2.2.4 Burst strength testing of hydrogel—The burst strengths (adhesive strengths) of various hydrogel formulations were tested using a custom-built mechanical burst tester following the standard protocol F2392-4 described by ASTM International [28]. Briefly, a sheet of tissue-mimicking collagenous substrate (sausage casing, Nippi Casing Co., Tokyo, Japan) with a 3-mm diameter hole bored at the center was mounted inside a polytetrafluoroethylene (PTFE) mold (3.0 cm in diameter); a 0.6 ml of the hydrogel precursor mix was deposited on the collagenous substrate confined by the PTFE mold to congeal. After incubating for a certain period of time (0.5, 1, 3, 6 and 8 hours, respectively) the hydrogel-substrate, in its entirety, was detached from the PTFE mold and mounted onto the pressurization unit of the tester. This was followed by activation of the syringe pump linked to the pressurization unit and a transducer, pressurization was initiated (at 2 ml/min) and the maximum pressure reached immediately prior to material failure was digitally recorded and registered on a computer. The burst pressure recorded as PSI was converted to mmHg using the following formula:

Pressure in mmHg/mm thickness= (Pressure in PSI X51) /Thickness (mm) of Hydrogel

2.2.5 Assessment hydrogel morphology by scanning electron microscopy— Fractured lyophilized pieces of Odex/teleostean/CEC hydrogels (0.5×0.5×0.2 cm^3) were secured on an aluminum board via copper tapes and they were sputtered with gold. Both surface and cross-sectional morphologies were captured with a field-emission scanning electron microscope (SFEG Leo 1550, AMO GmbH, Aachen, Germany) at 20 kV.

2.2.6 Swelling analysis—Swelling studies were performed on hydrogels in 0.01 M PBS at 37°C; the weights of the lyophilized hydrogels were recorded (W_d) prior to immersion in PBS. After 0.5, 2, 6, 24, 48 hours of incubation, the hydrogels were blotted with tissue paper to remove the excess water and weighed (W_s). The swelling ratio (q) was calculated by $q = (W_s\text{-}W_d)/W_d$.

2.2.7 Assessment of the cytotoxicity potential of hydrogel by a cell culture model—Cell toxicity assay was carried out in 96-well plates (1×10^5 cells/ml) on Odex/teleostean/CEC hydrogels and were performed in quintuplicate. The co-culture was performed using as a model cell line M. DUNNI mouse dermal fibroblast CRL-2017 cultured in a McCoy's 5A medium containing 10% FBS and 1% Pen-Strep solution, maintained at 37 °C under a humidified atmosphere of 5% CO_2. Cell viability studies were performed to verify the non-cytotoxicity of both hydrogels and their degradation byproducts using a MTS assay. In order to avoid any potential errors that could be caused by removal/manipulation of the hydrogel pieces while performing the assay, a non-contact methodology was employed to evaluate the cytotoxicity of the hydrogels. Briefly, sterilized hydrogel pieces, tailored to the dimension of approximately 2 mm×3 mm×2 mm, were first deposited in culture inserts and immersed in culture wells pre-seeded with cells (n = 3 per group). Monolayer cells were used as controls. Cell viabilities were determined on day 0, 3, 7, 14 and 28, respectively. At each time point, a 20 μl of MTS solution was added to the culture medium of each well, and monolayer cultured cells were used as controls. After incubating at 37 °C for 1 h, the absorbance of solutions were determined at 490 nm following manufacturer provided protocols.

2.2.8 In vitro degradation of hydrogels—After incubating for the time-spans ranging from 0 to 28 days, cell-laden hydrogels were retrieved at various time-points; their extents of degradation were determined by monitoring the hydrogels' weight losses.

2.2.9 Incorporation of rosiglitazone into hydrogels and demonstration of sustainable release—Rosiglitazone was incorporated into the 3XN hydrogel. In brief, 30 μl and 3 μl of a rosiglitazone stock solution (2 mg/ml dissolved in DMSO) were spiked into 1.5 ml of the 3XN hydrogel precursors, respectively; they were then lyophilized after congealing. The dried materials were cut into smaller pieces (5.0 mg each) and individually enclosed in dialysis tubings (MWCO 3,500); they were immersed in 10 ml aliquots of pH7.4 PBS in separate sample vials, incubated at 37°C under constant agitation at 50 RPM on an orbital shaker. At pre-determined time-points, 1 ml of sample was withdrawn from each vial and it was replenished with1 ml of fresh PBS. The rosiglitazone contents of the releasates were determined by HPLC (column: Waters Nova-Pak® C18, 150×3.9 mm; mobile phase: 30% acetonitrile in 40 mM NaH_2PO_4, 0.3 g SDS, 0.5 g EDTA, PH3.0; flow rate: 1.2 ml/min; temperature: 30°C; fluorescence detector: Waters 474; detection: ex245 nm/em367 nm). All tests were performed in triplicate.

2.2.10 in vivo efficacy of rosiglitazone released from hydrogel—The *in vivo* efficacy of rosiglitazone released from the hydrogel was assessed by a mouse (strain BALB/cj) subcutaneous implant model [22]. The study was performed according to the approved protocol (#1286) by the IACUC of SUNY-Stony Brook in compliance with the NIH guidelines for the care and use of laboratory animals (NIH Publication no. 85-23 Rev. 1985). Under the anesthesia of isoflurane (5% induction/2.5% maintenance), the sites for injection were prepped and sterilized with both betadine and isopropanol. The hydrogel precursor was prepared and transferred to a syringe with an 18G needle engaged. The needle was inserted subdermally and 0.5 ml of the content was slowly injected into the subdermal pouches dissected under gradual pressurization during injection. Likewise, rosiglitazone was incorporated into the hydrogel precursors (6.7 μg and 0.67 μg per 0.5 ml, respectively) for injection. The animals were euthanized after 14 days and the injection sites with the surrounding tissues were retrieved, fixed in 10% neutral buffered formalin, processed for paraffin sectioning, and stained with H&E.

The extent of cell/tissue-hydrogel interactions was determined by a blinded observer using a previously described methodology [29]. Infiltration of neutrophils, macrophages, mast cells and fibroblasts, indicative of inflammatory response, into the hydrogels was assessed qualitatively; the thickness of the fibrous tissue encapsulation was quantified in concert with analyzing the quality of the collagenous capsule. Briefly, on each specimen, twenty locations of hydrogel/capsule interfaces were randomly selected with images digitally captured at 20× magnification, the thickness of each capsule segment was manually measured by an arbitrary unit standardized for all specimens and the mean values were calculated. In addition, the cell density of each location was assessed by a semi-quantitative scale: minimal (1), slight (2), moderate (3), and high (4). The extents and qualities of collagen deposition were also assessed under polarization microscopy on a semi-quantitative scale: slight (+), moderate (++), and high (+++).

2.3 Statistical analysis

Data were analyzed by ANOVA to evaluate difference between groups. Post hoc comparison of means was accomplished with Student-Newman-Keuls test to determine significance between groups (α=0.05).

3. Results and discussion

CEC is ampiphilic with both -NH_2 and -COOH; partial oxidation of dextran converts some of its vicinal -OH into -CHO functionalities enabling it to serve as a macromolecular crosslinker for materials with free -NH_2; thus, Odex can crosslink both teleostean and CEC. Collectively, Odex, teleostean and CEC are very abundant in -OH, -COOH and -NH_2 groups and the reaction mixture is rich in highly interactive secondary and tertiary structures [30,31]. Blending of solutions of Odex, teleostean and CEC formed a transparent hydrogel quickly, this rapid gelation property was the result of the physical interactions of the secondary/tertiary structures, in concert with chemical crosslinkings via Schiff base formation between the -CHO on Odex and the -NH_2 on both the CEC and the teleostean. Theoretically, the disparity in the reaction times and the modes of interaction between the three components could result in the formation of multiple and interpenetrating networks (illustrated in Scheme 1). This study aimed to elucidate the mechanistic basis of multi-network hydrogel formation, demonstrated its non-cytotoxicity as well as the capacity for localized drug delivery.

3.1 Rheological analysis

Fig. 1 showed the temporal changes of the elastic modulus (G′) and the viscous modulus (G ″) of a typical hydrogel precursor formulation composed of 15% Odex/40% teleostean/5% CEC (in a ratio of 2:1:1). Initially, when G′ was lower than G″, the precursor exhibited the behavior of a viscous fluid. As both G′ and G″ elevated, the buildup rate of G′ appeared to be higher than that of G″ due to the interactions between the components. The differential buildup rates of G′ and G″ eventually led to a crossover ($t = t_{gel}$, the gel point) at approximately 200s, indicative of the transition of the Odex/teleostean/CEC system to a solid-phase. The relatively short t_{gel} also rendered this composition suitable for applications requiring *in situ* gelation. Both moduli eventually leveled off, implying the formation of a well-developed three-dimensional network.

The rheological behaviors of a series of partial formulations, Odex/CEC (ratio 1:1), Odex/teleostean (ratio 1:1) and teleostean/CEC (ratio 1:1), were tested in order to verify the multiple-network structure of the Odex/teleostean/CEC hydrogel. These precursors formed their corresponding single-network hydrogels, and their rheological profiles were depicted in Fig. 2. All partial formulations exhibited typical transitions of viscous liquids into solid hydrogels with their moduli increased gradually until plateauing; however, their corresponding t_{gel} and mechanical properties (reflected by G′) were vastly different; the results were summarized in Table 1. As shown in Fig. 2, the G′s of Odex/CEC and teleostean/CEC plateaued rapidly, implying prompt network formation. The results were also in good agreement with our previous investigation showing rapid and strong physical/chemical crosslinking of CEC by Odex [22]. Moreover, the existence of abundant -COOH and $-NH_2$ groups on the teleostean/CEC partial formulation enabled immediate formation of physical bonds (t_{gel}<30s), with the G′ plateau at 30 Pa after approximately 500s. Apparently, the teleostean/CEC hydrogel formed by physical crosslinking has relatively low mechanical strength. Compare to the relatively fast gelation times of both Odex/CEC and teleostean/CEC, the elevation rate of the G′ of the Odex/teleostean partial formulation was substantially slower, indicating its slow reaction rate. Its t_{gel} was approximately 2,500s and the G′ continued to elevate during the entire time span of testing. The buildup rate of the G′ of Odex/teleostean/CEC was slower than those of both Odex/CEC and teleostean/CEC but considerably faster than that of the Odex/teleostean, with a t_{gel} of 200s and its G′ continued to ascend after intersecting with that of the Odex/CEC system at about 3,000s. All the partial formulations were either weaker mechanically or had long t_{gel} or long reaction time span, thereby, posing certain limitations on their adaptabilities as *in situ* gelable hydrogels. In contrast, the Odex/teleostean/CEC hydrogel appeared to have assumed the collective characteristics of the three partial formulations via forming a triple-interpenetrating network.

3.2 Burst Pressure of hydrogels

The material cohesiveness of hydrogel, especially for those that are gelable *in situ*, is revealed by its burst strength [32–34]. Although the G′ deduced from the rheological analyses suggested that the Odex/teleostean/CEC system would be mechanically strong, its ultimate strength could not be efficiently elucidated due to the temporal limitation posed by conducting rheological analyses.

The temporal burst strengths of both the 3XN Odex/teleostean/CEC hydrogel and the three single-network binary partial formulations were determined by the custom-built tester according to ASTM protocol F2392-4. All hydrogels prepared were incubated at 37 °C for 0.5, 1, 3, 6 and 8 hours, respectively, prior to testing. The hydrostatic pressure exerted by the syringe pump increased continuously until the hydrogels failed, and the maximum (burst) pressure was digitally registered; the results were depicted in Fig. 3. The mechanical strength of teleostean/CEC was very weak due to its predominantly physical bondings (burst

strength <0.2 mmHg/mm, data not shown). The rates of elevation in burst strengths were in the order of Odex/CEC > Odex/teleostean/CEC > Odex/teleostean, mirroring their rheological profiles. After 0.5 hour, the burst strength of Odex/CEC reached its maximum at approximately 16 mmHg/mm thickness, indicating a fast reaction but relatively brittle and/or weak adhesion to substrate. The burst strength of Odex/teleostean rose steadily for 6 hours, with its ultimate burst strength registered at 44 mmHg/mm thickness, implicating a superior mechanical strength, high elasticity and strong adhesion to substrate. The buildup rate of the burst strength of the Odex/teleostean/CEC system was considerably faster than that of the Odex/teleostean; its burst strength surpassed that of the Odex/CEC by 1 hour, reaching a maximum of 65 mmHg/mm thickness after 3 hours. The burst strength of the Odex/teleostean/CEC hydrogel appeared to approximate the combined strengths of the three partial formulations. For comparison, fibrin glue was used as a benchmark and its strength was in the range of 14 mmHg/mm thickness. Collectively, the results of burst strength testing corroborated with those obtained from the rheological analyses demonstrating that the Odex/teleostean/CEC hydrogel was mechanically strong with a short t_{gel} and overall reaction time span.

3.3 Morphology of triple-network hydrogels

Typical Odex/teleostean/CEC hydrogels were translucent with a characteristic dark amber tint (not shown). Representative cross-sectional SEM images of lyophilized 3XN hydrogels along with those of the three single-network partial formulations were depicted in Fig. 4. All hydrogels formulations had porous and interconnected interior structures, but different in pore sizes and wall thickness. The physically crosslinked CEC/teleostean hydrogel exhibited the largest pore size (average: 500 μm) with thin wall amongst all formulations, corroborating with its weak mechanical strength. The Odex/CEC system had smaller pores attributable to its high crosslinking density; however, its loose sheet-like wall structure (due to its lower material content, at ~10%) implied a low mechanical strength of the hydrogel. Conversely, the pore structure of the Odex/teleostean/CEC hydrogel possessed thick wall, comparable to the structure of the Odex/teleostean hydrogel but more compact (average: 100 μm as compared to 250 μm of the latter). Since the Odex/teleostean/CEC hydrogel was comprised of a threefold interpenetrating network with high material content, it generally exhibited the smallest size pores with the greatest mechanical properties.

3.4 Interaction of fibroblast and 3XN hydrogels

The *in vitro* cytotoxicity potential of the 3XN hydrogels and cell-mediated degradation were evaluated by co-culturing them with dermal fibroblasts. Cells were seeded onto the hydrogels previously deposited on culture wells; wells without hydrogels were used as controls. Cell viabilities were examined at 0, 3, 7, 14, and 28 days by performing MTS assays and the results were depicted in Fig. 5. Short-term results (within 1 days) showed no significant difference between the cells incubated with the hydrogels and the controls, indicating the hydrogels did not have any adverse effect on cell growth, which could be inferred as material non-cytotoxicity. It was noticed on days 3 and 7 that the Odex/CEC hydrogel showed significantly lower cellular activity than the other two formulations ($p<0.05$), this could be attributed to the excessive negatively charged ($-COO^-$) residues present in the Odex/CEC matrix, which would not constitute a favorably environment for anchorage-dependent cells such as fibroblasts. Cells apparently continued to proliferate after 7 days; presumably, via deposition of extracellular matrix (ECM) and modification of the Odex/CEC hydrogels rendering it more amenable to cell growth [10]. Incorporation of teleostean into Odex/CEC to form the 3XN hydrogel greatly enhanced its cell-affinity. Collagen (thus, gelatin) is a major constituent of ECM and plays important roles on cell attachment, migration and proliferation [35]; adding teleostean ($-NH_2$ groups) also changed the negatively charged hydrogel network to a net positively charged network [36].

Therefore, the Odex/teleostean/CEC hydrogel constitutes an environment amenable to fibroblast growth. Additionally, longer term cell culture results (28 days) showed that the cells proliferated gradually with time and the magnitudes were comparable to those of the controls, which further confirmed the non-cytotoxic nature of the hydrogels. It could also be inferred that the degradation byproducts of the hydrogels were non-cytotoxic.

Degradation studies for the 3XN hydrogel in conjunction with the single network partial formulations were conducted under cell-mediated condition by monitoring their weight losses, the results were depicted in Fig. 6. Each hydrogel underwent relatively fast initial degradation followed by a more moderate phase after 2 weeks. The pace of degradation was in the order of Odex/CEC > Odex/teleostean > Odex/teleostean/CEC, suggesting a positive correlation between the stability and the crosslinking density. The gradual weight loss in concert with hydrogel fragmentation also suggested the steady breakdown of both crosslinks and polymer chains.

3.5 Release of rosiglitazone from 3XN hydrogels

Incorporation of rosiglitazone into the 3XN hydrogel did not affect its physical properties (t_{gel}, burst pressure, morphology, etc.) as rosiglitazone was simply pre-mixed into the precursor solution, and did not form the chemical or physical bonds with the hydrogel (data not shown). The rosiglitazone release kinetics from the hydrogels with two different drug loadings was depicted in Fig. 7. Approximately 65 and 80% of the rosiglitazone were released from the two formulations, respectively, after 2 weeks.

3.6 Assessment of the in vivo subcutaneous implant specimens

The hydrogel, per se, did not appear to have adversely affected the healing of the injection sites during the entire duration of implants, as suggested by the complete closures of the needle punctures which were consistent with similar types of wounds. The 3XN hydrogels were explanted two weeks after injection, the gross appearance of the hydrogel explants and the tissue adjoining the injection site did not show any signs of redness and edema indicating that the hydrogel did not induce extensive inflammatory response nor was there any evidence of tissue necrosis (not shown), further confirming the non-cytotoxicity of the hydrogel and its degradation byproducts. Fig. 8 depicted the representative histologies of the explanted tissues. The hydrogels were surrounded by fibrous capsules typically observed after material implantation; they also compared favorably with those implanted with poly-lactide-co-glycolide (i.e., Vicryl™, as positive controls) (not shown). Close examination of the histology specimens showed robust fibrous tissue formation around the 3XN hydrogel and extensive cell infiltration into it (Fig. 8A) with evidence of hydrogel degradation and tissue integration, as suggested by its partial disintegration along the periphery and assimilating with tissues. The extent of degradation/disintegration gradually diminished from the periphery towards the interior. This response expanded deep into the hydrogel's interior as indicated by the extent of penetration of cells. The hydrogel also showed greater resistance to *in vivo* degradation as compared to the partial formulation composed of CEC and Odex on comparable animal models [10,37,38]. Examination of the granulation tissue formed under polarized light showed collagen formation (Table 2).

Incorporation of rosiglitazone into the 3XN hydrogel profoundly changed its interaction with cells/tissues. One week after injection, bald spots had developed on the skin surrounding the injection sites (manifested as a bulge formed underneath the skin of each animal due to the containment of the hydrogel in the subdermal pouch) on 3 out of the 5 animals received the hydrogels containing 6.7 μg of rosiglitazone; whereas, the other 2 animals clearly had very thin hair on the skins surrounding their injection sites. Additionally, the needle puncture wounds were highly visible on all animals, suggesting delayed or

difficulty in healing. In contrast, the skin surrounding the injection sites on all the animals received the hydrogels containing 0.67 μg of rosiglitazone had moderate thinning of hairs; delayed/difficulty in healing of needle puncture was noticeable only on 1 animal. This observation suggested a dose-response effect. Analyses of the gross appearances of the explanted injection sites showed that the hydrogels were surrounded by thin (and flimsy) fibrous capsules (not shown). Close examination of the histology specimens of the tissues received 6.7 μg of rosiglitazone showed loose granulation tissue formation at the periphery of the hydrogel implant (Fig. 8B), strongly resembled that of typical very early stage (<5 days) healing in comparable animal models. Inflammatory cells were localized primarily at the periphery of the hydrogel indicating the lack of deep cell penetration. No collagen formation was noted under polarized light (Table 2). The capsules surrounding the hydrogels containing 0.67 μg of rosiglitazone were thicker with noticeable cell infiltration into the hydrogels from the peripheries (see Table 2). Overall, the effects it exerted on tissues were intermediate of the control and the hydrogel containing the higher dose of rosiglitazone.

Conclusion

A class of *in situ* gelable and mechanically strong triple-interpenetrating network (3XN) hydrogels, composed of minimally modified natural *GRAS* materials, oxidized dextran (Odex), *N*-carboxyethyl chitosan (CEC) and teleostean, has been formulated without the need of utilizing any potentially cytotoxic extraneous crosslinkers. The capacity of the 3XN hydrogel to serve as an injectable and biodegradable *in situ* gelable drug delivery vehicle for prolonged action was validated *in vivo* using rosiglitazone as a model drug. The lack of tissue necrosis implied that cell proliferation and tissue development are being inhibited instead of destroyed, and the extent of inhibition appears to be dose-related. Collectively, these results brings forth the possibility of incorporating rosiglitazone into the injectable 3XN hydrogel as an agent for modulating wound repair, leading to moderation of scar formation. Lastly, it should be noted that even though the current Odex/teleostean/CEC blend was able to form a solid hydrogel with good mechanical strength in the time span of minutes, a potential shortcoming for the current formulation is the relatively long time for it to achieve its maximum strength; however, we believe this could be shortened considerably through further optimization of the current formulations by properly adjusting the molecular weights of Odex and CEC, and their corresponding degrees of modification. We are currently conducting investigations to address this issue.

Acknowledgments

This study was supported by the National institutes of Health (AR056493); partial support was also provided an ECAT (Enhanced Center for Advanced Technology) grant from NYSTAR (New York Foundation for Science, Technology and Innovation) administered by the Center for Biotechnology of SUNY-Stony Brook. The author would like to thank Dr. Steve McClain (of McClain Laboratory, LLC) for his assistance in interpreting the histology; and Dr. Michael Crupain for assembling the burst strength tester.

References

1. Yan H, Nykanen A, Ruokolainen J, Farrar D, Gough JE, Saiani A, et al. Thermo-reversible protein fibrillar hydrogels as cell scaffolds. Faraday Discuss 2008;139:71–84. [PubMed: 19048991]
2. Zeng Q, Chen W. The functional behavior of a macrophage/fibroblast co-culture model derived from normal and diabetic mice with a marine gelatin-oxidized alginate hydrogel. Biomaterials 2010;31(22):5772–81. [PubMed: 20452666]
3. Chau Y, Luo Y, Cheung AC, Nagai Y, Zhang S, Kobler JB, et al. Incorporation of a matrix metalloproteinase-sensitive substrate into self-assembling peptides - a model for biofunctional scaffolds. Biomaterials 2008;29(11):1713–19. A. [PubMed: 18192002]

4. Schmidt JJ, Rowley J, Kong HJ. Hydrogels used for cell-based drug delivery. J Biomed Mater Res A 2008;87(4):1113–22. [PubMed: 18837425]
5. Zhang J, Chen H, Xu L, Gu Y. The targeted behavior of thermally responsive nanohydrogel evaluated by NIR system in mouse model. J Control Release 2008;131(1):34–40. [PubMed: 18691619]
6. Huynh DP, Nguyen MK, Pi BS, Kim MS, Chae SY, Lee KC, et al. Functionalized injectable hydrogels for controlled insulin delivery. Biomaterials 2008;29(16):2527–34. [PubMed: 18329707]
7. Kim J, Park Y, Tae G, Lee KB, Hwang SJ, Kim IS, et al. Synthesis and characterization of matrix metalloprotease sensitive-low molecular weight hyaluronic acid based hydrogels. J Mater Sci Mater Med 2008;19(11):3311–8. [PubMed: 18496734]
8. Liao H, Zhang H, Chen W. Differential physical, rheological, and biological properties of rapid *in situ* gelable hydrogels composed of oxidized alginate and gelatin derived from marine or porcine sources. J Mater Sci Mater Med 2009;20(6):1263–71. [PubMed: 19184370]
9. Weng LH, Pan H, Chen W. Self-crosslinkable hydrogels composed of partially oxidized hyaluronan and gelatin: *in vitro* and *in vivo* responses. J Biomed Mater Res A 2008;85A:352–65. [PubMed: 17688243]
10. Weng L, Romanov A, Rooney J, Chen W. Non-cytotoxic, *in situ* gelable hydrogels composed of N-carboxyethyl chitosan and oxidized dextran. Biomaterials 2008;29(29):3905–13. [PubMed: 18639926]
11. Bodugoz-Senturk H, Macias CE, Kung JH, Muratoglu OK. Poly(vinyl alcohol)-acrylamide hydrogels as load-bearing cartilage substitute. Biomaterials 2009;30(4):589–96. [PubMed: 18996584]
12. Cho E, Kutty JK, Datar K, Soo Lee J, Vyavahare NR, Webb K. A novel synthetic route for the preparation of hydrolytically degradable synthetic hydrogels. J Biomed Mater Res A 2008;90(4): 1073–82. [PubMed: 18671270]
13. Pratoomsoot C, Tanioka H, Hori K, Kawasaki S, Kinoshita S, Tighe PJ, et al. A thermoreversible hydrogel as a biosynthetic bandage for corneal wound repair. Biomaterials 2008;29(3):272–81. [PubMed: 17976717]
14. Liu Y, Chan-Park MB. Hydrogel based on interpenetrating polymer networks of dextran and gelatin for vascular tissue engineering. Biomaterials 2009;30(2):196–207. [PubMed: 18922573]
15. Ta HT, Dass CR, Dunstan DE. Injectable chitosan hydrogels for localised cancer therapy. J Control Release 2008;126(3):205–16. [PubMed: 18258328]
16. Kopecek J. Hydrogel biomaterials: a smart future? Biomaterials 2007;28(34):5185–92. [PubMed: 17697712]
17. Weng L, Gouldstone A, Wu Y, Chen W. Mechanically strong double network photocrosslinked hydrogels from N,N-dimethylacrylamide and glycidyl methacrylated hyaluronan. Biomaterials 2008;29(14):2153–63. [PubMed: 18272215]
18. Kuo CK, Ma PX. Ionically crosslinked alginate hydrogels as scaffolds for tissue engineering: part 1. Structure, gelation rate and mechanical properties. Biomaterials 2001;2(6):511–21. [PubMed: 11219714]
19. Yasuda K, Ping Gong J, Katsuyama Y, Nakayama A, Tanabe Y, Kondo E, et al. Biomechanical properties of high-toughness double network hydrogels. Biomaterials 2005;26(21):4468–75. [PubMed: 15701376]
20. Tirumala VR, Tominaga T, Lee S, Butler PD, Lin EK, Gong JP, et al. Molecular model for toughening in double-network hydrogels. J Phys Chem B 2008;112(27):8024–31. [PubMed: 18558754]
21. Tanabe Y, Yasuda K, Azuma C, Taniguro H, Onodera S, Suzuki A, et al. Biological responses of novel high-toughness double network hydrogels in muscle and the subcutaneous tissues. J Mater Sci Mater Med 2008;19(3):1379–87. [PubMed: 17914620]
22. Weng L, Chen X, Chen W. Rheological characterization of *in situ* crosslinkable hydrogels formulated from oxidized dextran and N-carboxyethyl chitosan. Biomacromolecules 2007;8(4): 1109–15. [PubMed: 17358076]
23. Nowakowska M, Zapotoczny S, Sterzel M, Kot E. Novel water-soluble photosensitizers from dextrans. Biomacromolecules 2004;5:1009–14. [PubMed: 15132694]

24. Mehvar R. Dextrans for targeted and sustained delivery of therapeutic and imaging agents. J Control Release 2000;69:1–25. [PubMed: 11018543]
25. Ferdous A, Akaike T, Maruyama A. Inhibition of sequence-specific protein-DNA interaction and restriction endonuclease cleavage via triplex stabilization by poly(L-lysine)- graft-dextran copolymer. Macromolecules 2004;37:3239–48.
26. Draye JP, Delaey B, Van de Voorde A, Van Den Bulcke A, Bogdanov B, et al. *In vitro* release characteristic of bioactive molecules from dextran dialdehyde crosslinked gelatin hydrogels films. Biomaterials 1998;19:99–107. [PubMed: 9678856]
27. Mao-Qiang M, Fowler AJ, Schmuth M, Lau P, Chang S, Brown BE, et al. Peroxisome-proliferator-activated receptor (PPAR)-gamma activation stimulates keratinocyte differentiation. J Invest Dermatol 2004;123(2):305–12. [PubMed: 15245430]
28. Jiang H, Wang Y, Huang Q, Li Y, Xu C, Zhu K, et al. Biodegradable hyaluronic acid/N-carboxyethyl chitosan/protein ternary complexes as implantable carriers for controlled protein release. Macromol Biosci 2005;5:1226–33. [PubMed: 16307434]
29. De Jong WH, Dormans JA, Van Steenbergen MJ, Verharen HW, Hennink WE. Tissue response in the rat and the mouse to degradable dextran hydrogels. J Biomed Mater Res A 2007;83(2):538–45. [PubMed: 17530632]
30. Van Tomme SR, Van Steenbergen MJ, De Smedt SC, Van Nostrum CF, Hennink WE. Self-gelling hydrogels based on oppositely charged dextran microspheres. Biomaterials 2005;26(14):2129–35. [PubMed: 15576188]
31. Van Tomme SR, Hennink WE. Biodegradable dextran hydrogels for protein delivery applications. Expert Rev Med Devices 2007;4(2):147–64. [PubMed: 17359222]
32. Kobayashi H, Sekine T, Nakamura T, Shimizu Y. *In vivo* evaluation of a new sealant material on a rat lung air leak model. J Biomed Mater Res 2001;58(6):658–65. [PubMed: 11745518]
33. Shazly TM, Artzi N, Boehning F, Edelman ER. Viscoelastic adhesive mechanics of aldehyde-mediated soft tissue sealants. Biomaterials 2008;29(35):4584–91. [PubMed: 18804861]
34. Wallace DG, Cruise GM, Rhee WM, Schroeder JA, Prior JJ, Ju J, et al. A tissue sealant based on reactive multifunctional polyethylene glycol. J Biomed Mater Res 2001;58(5):545–55. [PubMed: 11505430]
35. Badylak SF. The extracellular matrix as a scaffold for tissue reconstruction. Semin Cell Dev Biol 2002;13:377–83. [PubMed: 12324220]
36. Zhang R, Tang M, Bowyer A, Eisenthal R, Hubble J. A novel pH- and ionic-strength-sensitive carboxy methyl dextran hydrogel. Biomaterials 2005;26(22):4677–83. [PubMed: 15722138]
37. Yuan Z, Zakehaleva J, Ren H, Liu J, Chen W, Pan Y. Noninvasive and High-resolution Optical Monitoring of Healing of Diabetic Dermal Excisional Wounds Implanted with Biodegradable *in situ* Gelable Hydrogels. Tissue Eng Part C Methods 2010;16(2):237–47. javascript:AL get(this, 'jour', 'Tissue Eng Part C Methods.'). [PubMed: 19496703]
38. Falabella CA, Melendez M, Weng LH, Chen W. Novel macromolecular crosslinking hydrogel to reduce intra-abdominal adhesions. J Surg Res 2010;159(2):772–8. [PubMed: 19481223]

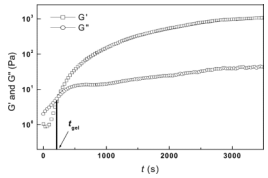

Fig.1.

Time evolution of the storage modulus (G′) and the loss modulus (G″) for a triple network hydrogel formulation composed of 15% Odex/40% teleostean/5% CEC (ratio 2:1:1). G′ and G″ crossover is denoted as t_{gel} (gelation point)

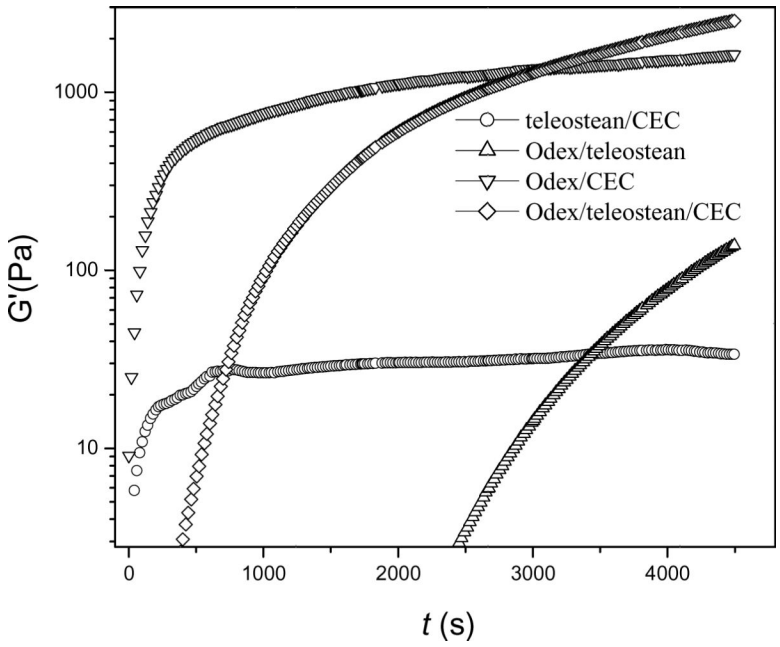

Fig.2.

Time evolution of the elastic moduli (G′) and the loss moduli (G″) of the triple-network hydrogel and the corresponding single-networked partial formulations The concentrations of Odex, teleostean and CEC solutions are 15, 40 and 5%, respectively.

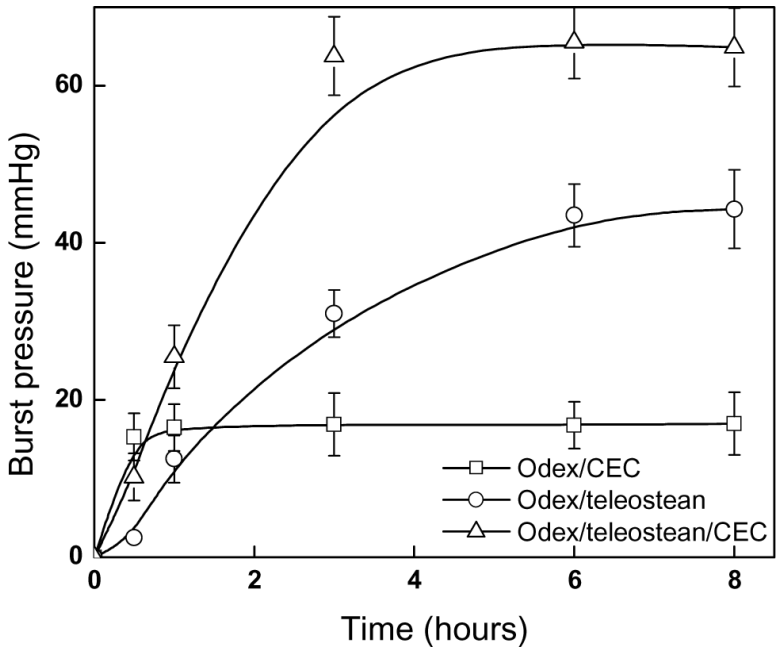

Fig.3.
Time evolution of burst pressure

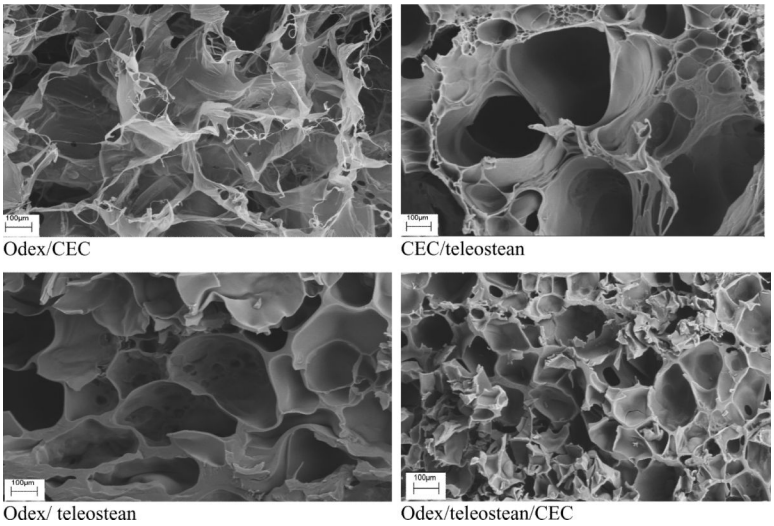

Fig.4.
SEM images of lyophilized hydrogels

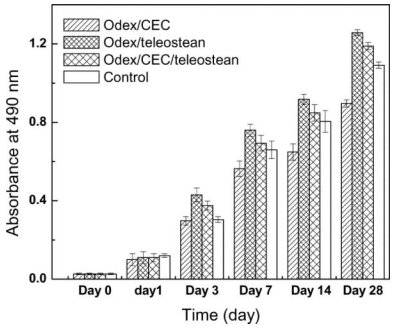

Fig.5.
Relative viabilities on cells seeded on various hydrogel formulations

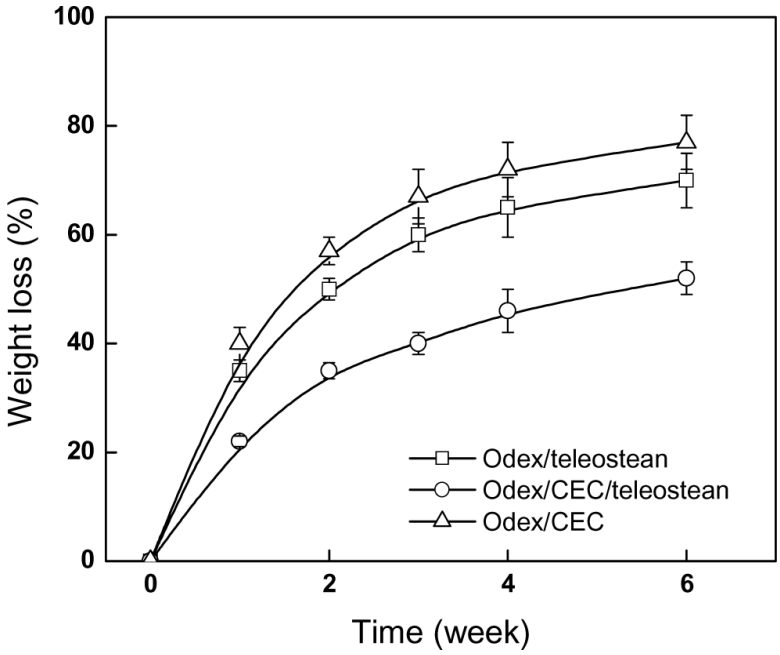

Fig.6.
Degradation of hydrogels in fibroblast cell culture model

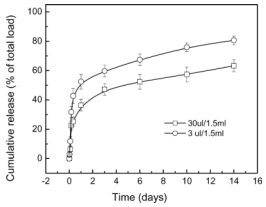

Fig.7.
Release of rosiglitazone from hydrogel with different drug loadings

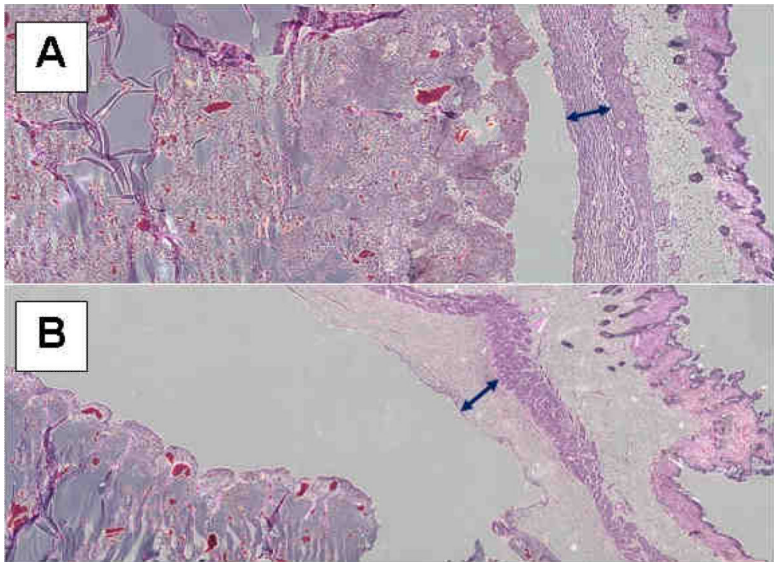

Fig.8.

Tissue sections of implanted hydrogels: (A) no rosiglitazone, and (B) 6.7 μg of rosiglitazone incorporated

The capsule (denoted by ↔) surrounding the hydrogel containing no rosiglitazone (A) is considerably denser than its counterpart with rosiglitazone. In the absence of rosiglitazone, cells penetrated deep into the hydrogel and it showed extensive degradation and signs of gradual integration with tissue leading to moderate shrinkage of the partially degraded hydrogel during histology processing. Shrinkage of the hydrogel during histology preparation leading to its detachment from the tissue was self-evident. In contrast, the presence of rosiglitazone (B) limited cell penetration and greatly moderated the extent of hydrogel degradation, as reflected by the largely intact hydrogel and its greater degree of shrinkage

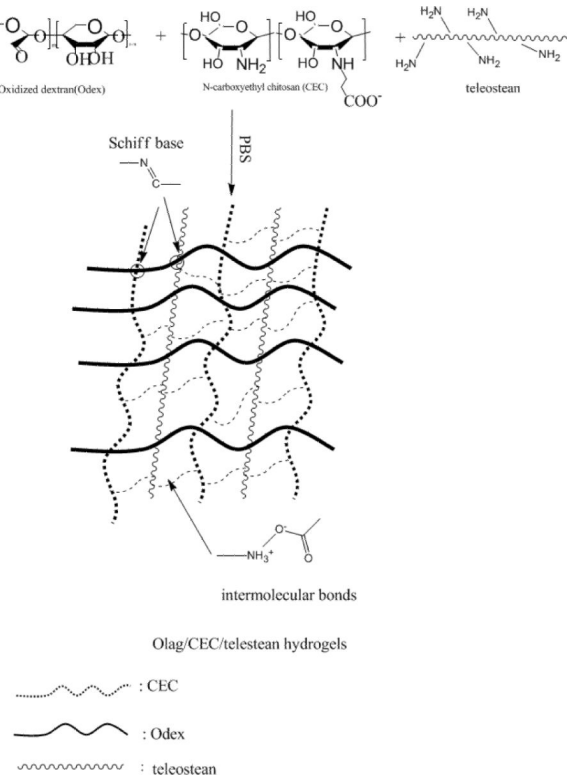

Scheme 1.
Schematic representation of the formation of the triple-network hydrogel

Table 1

The t_{gel}'s of hydrogels at 37°C

Sample	Odex/CEC	Odex/ teleostean	CEC/ teleostean	Odex/CEC/ teleostean
Weight ratio	1/1	1/1	1/1	2/1/1
t_{gel} (s)	100	2550	<30	200

The concentrations of Odex, teleostean and CEC solutions are 15, 40 and 5%, respectively.

Table 2

Dose-response effect on the fibrous tissues surrounding the implanted hydrogels containing rosiglitazone.

Rosiglitazone Dose	Capsule Density	Average Capsule Thickness	Collagen Deposition
0	3.0±0	10.9±3.0 (range: 7.4 to 12.0)	+++
0.67 μg	2.2±0.5	7.7±1.1 (range: 6.1 to 8.6)	+
6.7 μg	1.5±0.5	7.2±1.5 (range: 5.9 to 9.3)	None